Inclusive negative-hadron production from high-energy $\bar{\nu}$-nucleus charged-current interactions

J. P. Berge, D. Bogert, R. Endorf,* R. Hanft, J. A. Malko, G. Moffatt,* F. A. Nezrick, W. Scott,† W. Smart, and J. Wolfson

Fermi National Accelerator Laboratory, Batavia, Illinois 60510

V. V. Ammosov, A. H. Amrakhov, A. G. Denisov, P. F. Ermolov, V. A. Gapienko, V. I. Klukhin, V. I. Koreshev, P. V. Pitukhin, V. G. Rjabov, E. A. Slobodyuk, and V. I. Sirotenko

Institute of High Energy Physics, Serpukhov, USSR

V. I. Efremenko, P. A. Gorichev, V. S. Kaftanov, V. D. Khovansky, G. K. Kliger, V. Z. Kolganov, S. P. Krutchinin, M. A. Kubantsev, A. N. Rosanov, M. M. Savitsky, and V. G. Shevchenko

Institute of Theoretical and Experimental Physics, Moscow, USSR

C. T. Coffin, R. N. Diamond,‡ H. French,§ W. Louis, B. P. Roe, R. T. Ross,† A. A. Seidl, and D. Sinclair

University of Michigan, Ann Arbor, Michigan 48109

(Received 5 May 1978)

We present data on inclusive negative-hadron production from charged-current antineutrino interactions in a 21% Ne–H mixture. Inclusive single-particle distributions are presented and are shown to be insensitive to the momentum transferred to the hadron vertex. Comparisons made to inclusive data from $\pi^- p$ and $\pi^- n$ interactions indicate a close similarity between the hadrons resulting from π-nucleon and $\bar{\nu}$-nucleus interactions. The general features of the $\bar{\nu}$-nucleus data are found to be similar to those seen in $\bar{\nu}p$ interactions. This last observation implies that $\bar{\nu}p$ and $\bar{\nu}n$ interactions are similar and that nuclear effects are small.

I. INTRODUCTION

Measurements of inclusive hadron production in neutrino- and antineutrino-induced reactions play a crucial role in our understanding of hadron production in a large class of related processes. In this paper we report on a study of inclusive negative hadron production by antineutrinos, carried out using the Fermilab 15-ft bubble chamber filled with a 21% atomic neon-hydrogen mixture. With this mixture 16% of the interactions are off free hydrogen targets.

Muon inclusive distributions (x and y distributions) for the reaction $\bar{\nu}_\mu + \text{nucleus} \rightarrow \mu^+ + \text{hadrons}$ as measured in this experiment have been published in a separate paper.[1] The data were based on approximately 600 events in the energy range 10–200 GeV. The data presented here are based on the same event sample and the procedures and criteria employed in the analysis are identical: Events are included in the sample if they have a positive muon, identified by the External Muon Identifier (EMI),[2] with momentum greater than 4 GeV/c, and if the energy transfer to the hadrons measured in the laboratory is greater than 2.0 GeV.

In this experiment it is in general not possible to make an unambiguous mass assignment for the charged hadrons except at very low momentum (<1 GeV/c). For the negative tracks the majority (>90%) are pions, and for this analysis all negative

tracks have been assigned a pion mass. The positive tracks include some unidentified protons which could obscure the interpretation of the results if they were systematically assigned the wrong mass hypothesis. For this reason distributions for positive hadrons are not shown.

II. EXPERIMENTAL RESULTS

We have analyzed the inclusive negative hadron h^- production in terms of the variables W^2, Q^2, P_t^2, P_{out}^2, $Z = E_{(h^-)}/E_{\text{had}}$, and $X_F = 2P_{\parallel}^*/W$. Here W is the total hadronic energy, P_t and $P_{\parallel}^*$ are the transverse and longitudinal h^- momentum, respectively, all calculated in the hadronic rest frame; $E_{(h^-)}$ and E_{had} are the h^- energy and total hadronic energy calculated in the laboratory system; Q^2 is the square of the four-momentum transfer between the $\bar{\nu}$ and μ^+; P_{out} is the h^- momentum perpendicular to the $\bar{\nu}\mu^+$ production plane. The variables X_F, W^2 and P_t^2 so defined are common to inclusive studies using hadron beams.

Figures 1(a) and 1(b) show, respectively, the W^2 and Q^2 distributions for our data sample. We note that although W^2 goes out to values greater than 80 GeV^2, the average W^2 is much lower, approximately 15 GeV^2. (For a pion-nucleon interaction this W^2 corresponds to an ~8 GeV/c incident pion momentum.) Thus, in terms of the hadronic energy, these data are in a comparatively
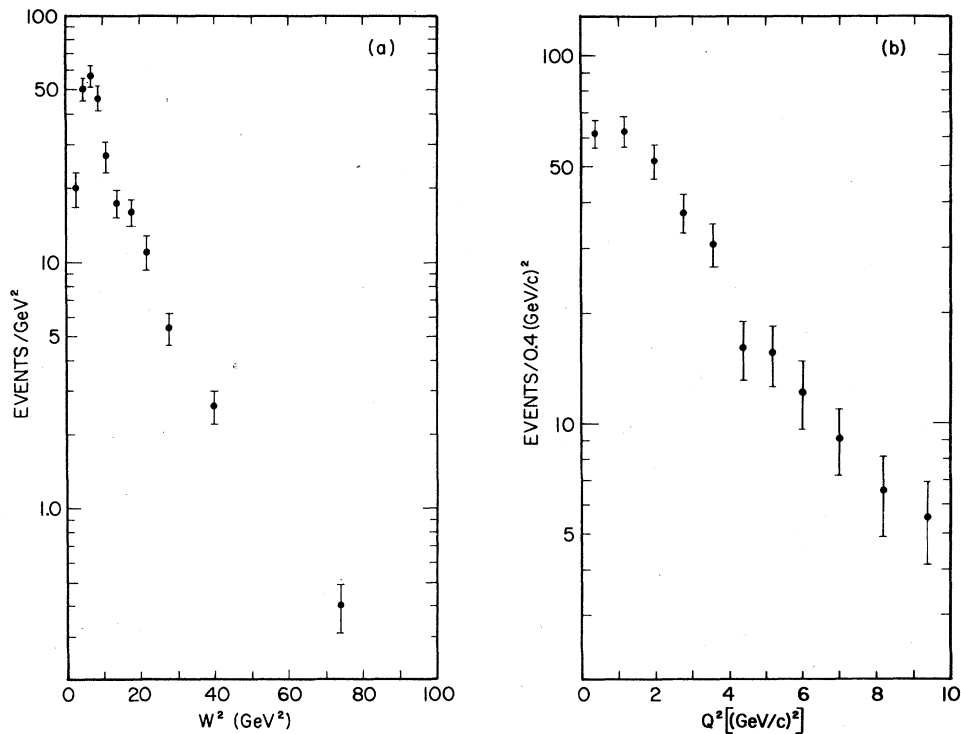
FIG. 1. Distribution of (a) W^2 and (b) Q^2 for the selected $\bar{\nu}$-nucleus charged-current events.

low-energy region.

Figure 2(a) shows the average h^- multiplicity as a function of $\ln W^2$. The data appear to be linear in $\ln W^2$; the solid line in Fig. 2(a) is the result of a fit to a linear form $A + B \ln W^2$ and yields $\langle h^- \rangle = (-0.25 \pm .03) + (0.76 \pm 0.01) \ln W^2$ in the $4 < W^2$

< 100 GeV^2 region ($\chi^2/\mathrm{ND} = 4.2/10$). This linear behavior is not significantly dependent on Q^2. Fits to the same linear form yield parameters $A = -0.17 \pm 0.18$, $B = 0.69 \pm 0.09$ in the region $Q^2 < 2$ (GeV/c)^2 and $A = -0.05 \pm 0.19$, $B = 0.71 \pm 0.08$ in the region $2 < Q^2 < 10$ (GeV/c)^2. For comparison
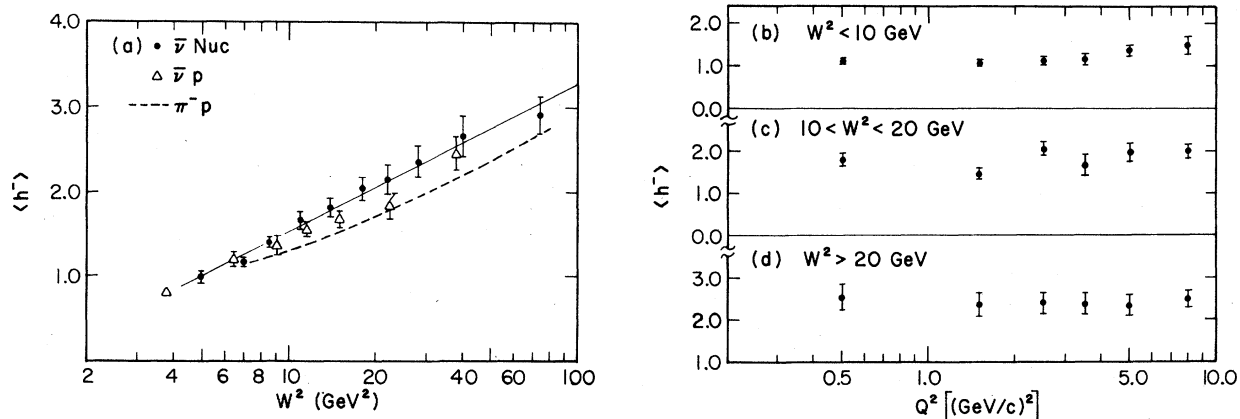

FIG. 2. Distribution of $\langle h^- \rangle$ with respect to (a) W^2 and in (b), (c), and (d) Q^2, in different intervals of W^2. In (a) comparisons are made with $\bar{\nu}p$ data (triangular points) and $\pi^- p$ data (dashed curve). The solid line is a fit to an $A + B \ln W^2$ term.
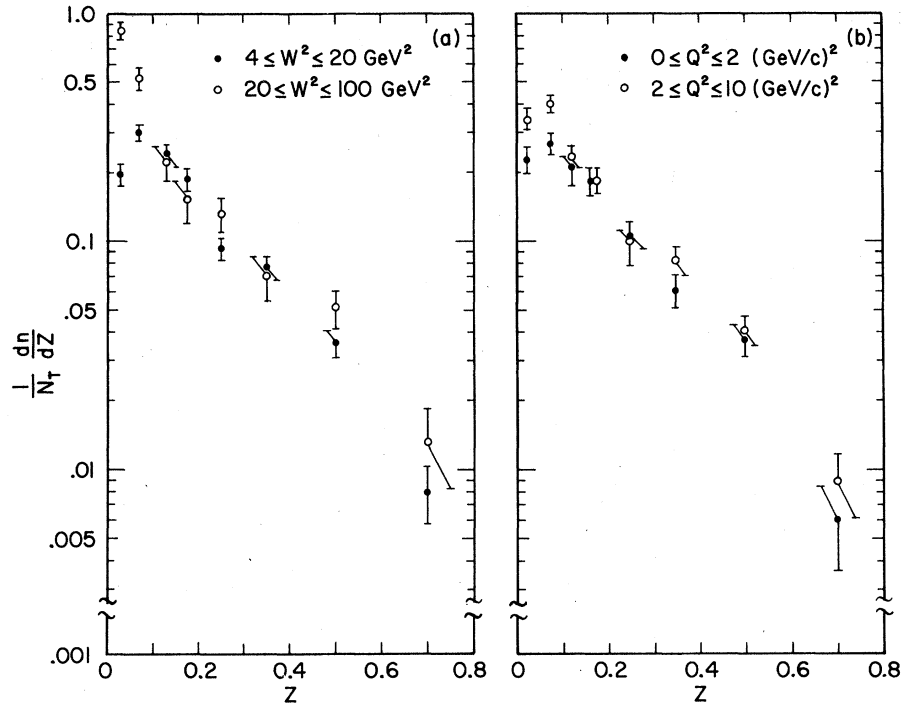
FIG. 3. Normalized Z distributions for (a) two Q^2 regions and (b) two W^2 regions.
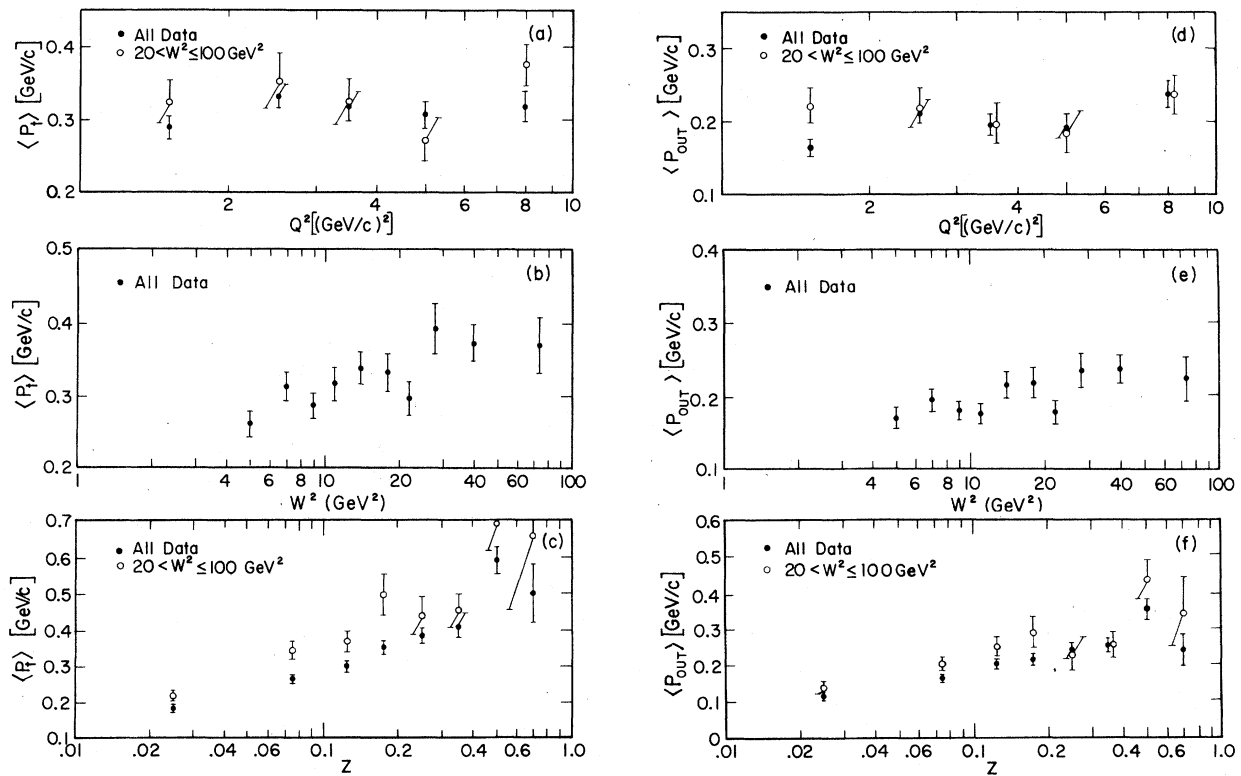
FIG. 4. Distribution of $\langle P_t \rangle$ with respect to (a) Q^2, (b) W^2, and (c) Z. The same distributions for $\langle P_{out} \rangle$ are shown in (d), (e), and (f), respectively.

the triangles in Fig. 2(a) show the $\langle h^- \rangle$ distribution obtained from $\bar{\nu}p$ interactions.[3] Since the weak current transfers a negative charge to the target nucleon we have compared our data in Fig. 2(a) to data obtained from $\pi^- p$ interactions (dashed curve).[4] We note that the $\langle h^- \rangle$ distributions for both the $\bar{\nu}p$ and $\pi^- p$ data appear to be slightly lower than the $\bar{\nu}$ nucleus data. This may be explained in part by the fact that in the $\bar{\nu}$ nucleus data there are both neutron and proton targets, and the $\langle h^- \rangle$ multiplicity is somewhat higher for a neutron target.[5]

In contrast to the observed dependence of $\langle h^- \rangle$ on W^2, we see in Figs. 2(b)–2(d) that $\langle h^- \rangle$ is weakly dependent on Q^2 with only a possible small dependence in the low-W^2 region. This small Q^2 dependence is in agreement with results obtained from $\bar{\nu}p$ data.[3]

In Figs. 3(a) and 3(b) are presented the normalized Z distributions for two W^2 and two Q^2 regions, respectively. In the quark parton model high-Z particles are fragments from one quark only and are predicted to be independent of Q^2 and W^2. The distributions in Fig. 3 are consistent with this interpretation, although the onset of this scaling behavior at such small Z values is probably fortuitous.

The dependence of $\langle P_t \rangle$ on Q^2, W^2, and Z is shown in Figs. 4(a), 4(b), and 4(c), respectively. We see that $\langle P_t \rangle$ is independent of Q^2. This independence has been seen previously in $\bar{\nu}$, ν, and e scattering.[3,6,7] The distribution of $\langle P_t \rangle$ vs W^2 [Fig. 4(b)] exhibits a slow rise with increasing W^2 and perhaps a plateau at high W^2. The distribution of $\langle P_t \rangle$ vs Z [Fig. 4(c)] rises with increasing Z, the dependence appearing to be approximately linear in $\ln(Z)$. We present in Figs. 4(d)–4(f) the distributions of $\langle P_{out} \rangle$ as a function of Q^2, W^2, and Z. The $\langle P_{out} \rangle$ distributions have the same qualitative dependences as those for $\langle P_t \rangle$. The $\langle P_t \rangle$ distributions of Fig. 4 are in general agreement with the results from inclusive $\bar{\nu}p$ data[3] and inclusive hadron data. We note, however, that the $\bar{\nu}p$ data appear to show the onset of a plateau in $\langle P_t \rangle$ vs Z at $Z \approx 0.3$ which is not indicated by the data in Fig. 4(c). Although the errors are large, Fig. 4(c) is consistent with $\langle P_t \rangle$ being independent of W^2 in the high-Z region.

Figure 5 shows the P_t^2 distribution of the inclusive h^- sample for all the data and for the subsamples having $4 < W^2 < 20$ GeV^2 and $20 < W^2 < 100$ GeV^2. We have fit these distributions in the range $0.0 \leqslant P_t^2 < 1.0$ (GeV/c)^2 to the form $dN/dP_t^2 = Ae^{-BP_t}$, obtaining B values of 6.54 ± 0.20 (GeV/c)$^{-1}$ ($\chi^2/$ND $= 8.4/5$) and $5.81 \pm .40$ (GeV/c)$^{-1}$ ($\chi^2/$ND $= 1.9/5$) for $4 \leqslant W^2 < 20$ GeV^2 and $20 \leqslant W^2 < 100$ GeV^2, respectively. We note that the data
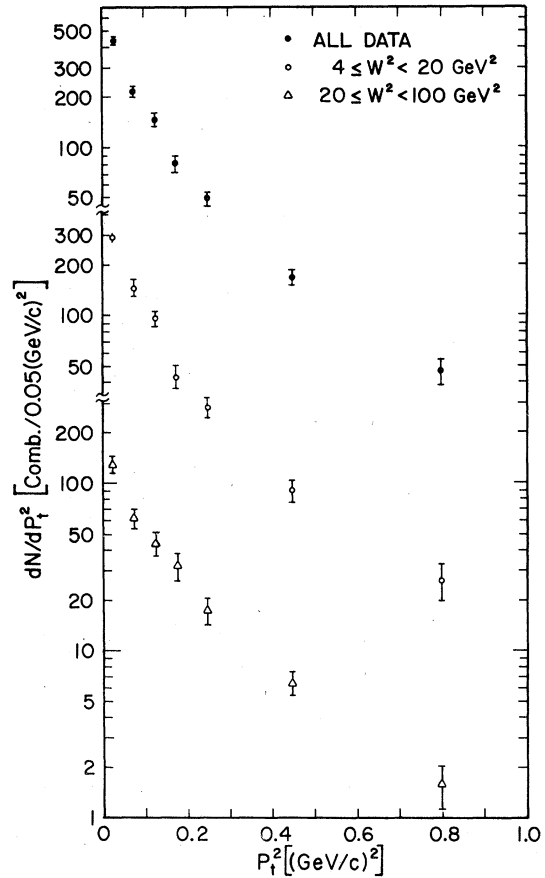

FIG. 5. Distribution of P_t^2 for total data and two W^2 regions.

in general give poorer fits[8] to the form $dN/dP_t^2 = Ae^{-BP_t^2}$. This latter form was used to parameterize the inclusive hadronic distributions in the $\bar{\nu}p$ data of Ref. 3.

To study the Feynman-scaling behavior of the inclusive h^- data we define the invariant structure function $f_1(X_F)$ by

$$f_1(X_F) = \frac{1}{N_{tot}} \int \frac{E^*}{\sqrt{W^2}} \frac{d^2n}{dX_F dP_t^2} dP_t^2 \; ,$$

where E^* is the h^- energy in the hadron rest frame, N_{tot} is the total number of events, and n is the number of h^- tracks. The distributions of f_1 for two W^2 and two Q^2 regions are shown in Figs. 6(a) and 6(b), respectively. In the nomenclature of strong-interaction physics Feynman scaling manifests itself as the independence of f_1 with respect to the total hadronic energy W. As seen from Fig. 6(a), the invariant structure function $f_1(X_F)$ shows no strong W^2 dependence when compared between the regions $4 < W^2 < 20$ GeV^2 and $20 < W^2 < 100$ GeV^2. Likewise, the f_1 distributions
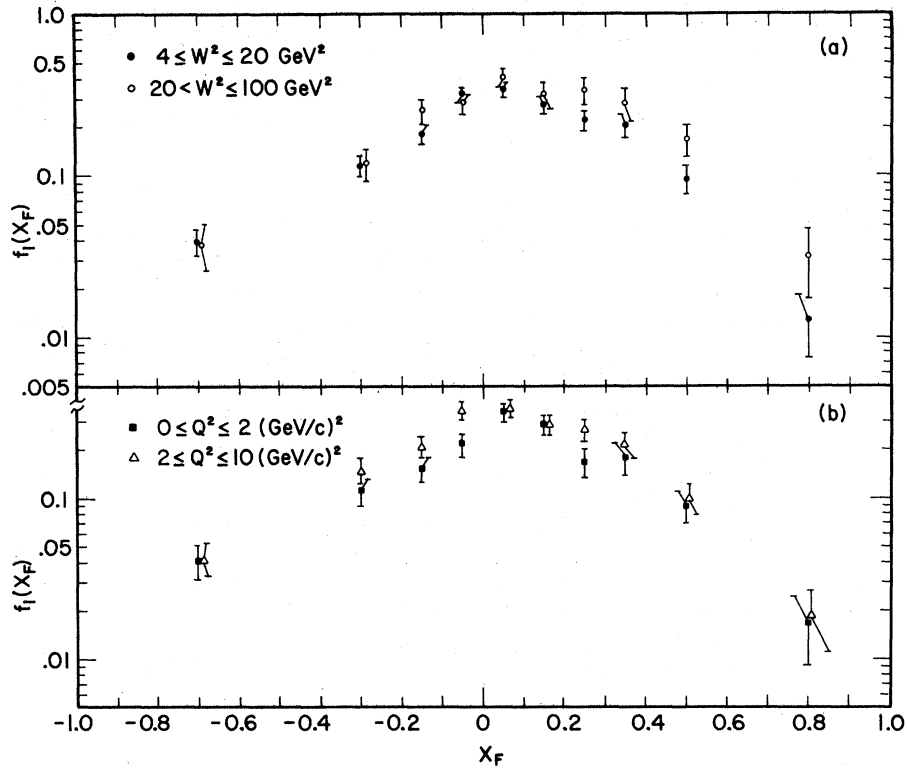
FIG. 6. Distribution of $f_1(X_F)$ for (a) two W^2 regions and (b) two Q^2 regions.
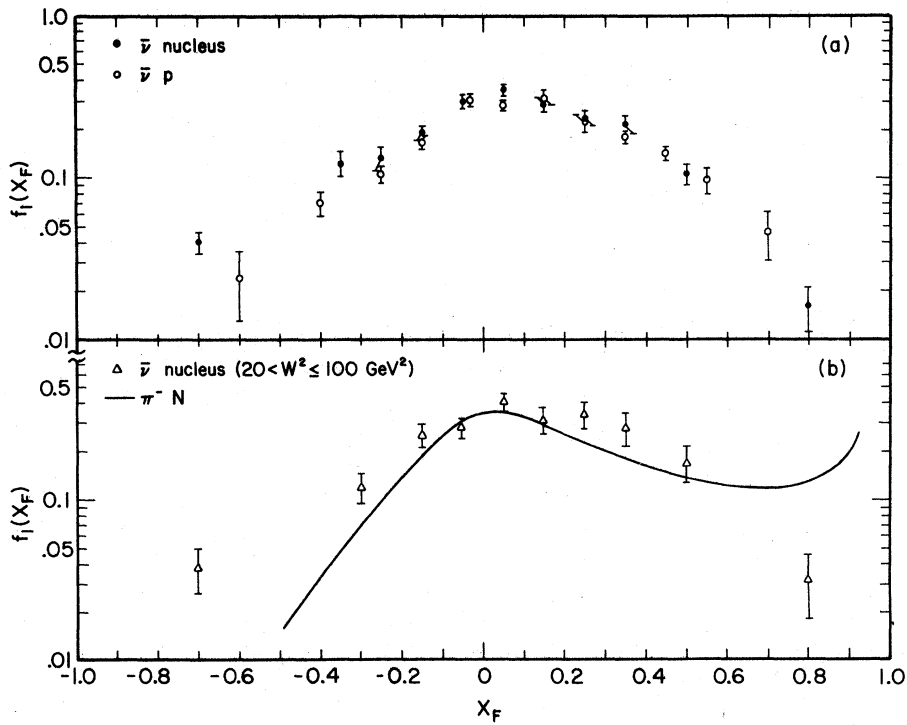
FIG. 7. (a) Comparison of $f_1(X_F)$ for $\bar{\nu}$ nucleus interactions (solid data points) and $\bar{\nu}p$ interactions (Ref. 3) (open data points). (b) Comparison of $f_1(X_F)$ from $\bar{\nu}$ nucleus interactions and π^-p (Ref. 9) plus π^-n (Ref. 10) interactions.

in Fig. 6(b) show no significant Q^2 dependence. The absence of a strong W^2 dependence for f_1 is perhaps not surprising. The average W^2 for the $4 < W^2 < 20$ GeV^2 and $20 < W^2 < 100$ GeV^2 regions is ~10 and ~35 GeV^2, respectively. In a comparison[9] of $f_1(X_F)$ between an s of 16 and 35 GeV^2, obtained from $\pi^- p$ data, it was found that $f_1(X_F)$ varied by less than ~10% in the region $-0.6 < X_F < 0.6$.

In Fig. 7 we have compared our $f_1(X_F)$ distributions with those obtained from other experiments. Figure 7(a) shows the distribution of $f_1(X_F)$ for our total data sample (solid circles) and the same distribution obtained from the $\bar{\nu}p \to \mu^+ h^- X$ interaction.[3] The two distributions are in excellent agreement over almost the entire X_F range.

In Fig. 7(b) we have replotted the $f_1(X_F)$ distribution for the $20 < W^2 < 100$ GeV^2 region. We have compared this distribution to $\pi^- p$ (Ref. 8) and $\pi^+ p$ data[10] (i.e., charge conjugate of $\pi^- n$) having $s \sim 35$ GeV^2, since this s value corresponds to the average W^2 in the 20–100 GeV^2 region. In the 21% neon-hydrogen mixture there are 1.4 proton targets for each neutron. Since the $\bar{\nu}$ interacts off u-type quarks, we have added the $\pi^- p$ and $\pi^- n$ data with the relative weights $(1.4 \times 2)f_1(\pi^- p) + f_1(\pi^- n)$. The result is shown by the solid curve in Fig. 7(b), where the data have been normalized at $X_F = 0.0$. We note that the hadron data show a characteristic

forward peak (leading-particle effect) which is not observed in the antineutrino data. Except in the large-$|X_F|$ regions the shapes of the hadron and antineutrino data are in reasonable agreement.

III. CONCLUSIONS

We find that in general the overall properties of the inclusive h^- data obtained from $\bar{\nu}$-nucleus interactions are similar to those obtained from inclusive π-nucleon data. In addition the inclusive h^- distributions are found to be insensitive to the momentum transferred to the hadronic vertex. These results imply that in $\bar{\nu}$ interactions the hadronic vertex has only a small "memory" of the details of the leptonic vertex. In the 21% Ne–H mixture used in this exposure 42% of the target nucleons are neutrons in the Ne nuclei. The similarities observed between the $\bar{\nu}$ interactions in this Ne–H mix and $\bar{\nu}$ interactions in hydrogen imply that $\bar{\nu}p$ and $\bar{\nu}n$ interactions are similar and that nuclear effects in our data are small compared to our statistical errors.

ACKNOWLEDGMENT

---

*Permanent address: University of Cincinnati, Cincinnati, Ohio 45221.

†Present address: CERN, 1211 Geneva 23, Switzerland.

‡Present address: Florida State University, Tallahassee, Florida 32306.

§Present address: Columbia University, New York, New York 10027.

[1] Fermilab-IHEP-ITEP-Michigan Neutrino Group, Phys. Rev. Lett. **39**, 382 (1977).

[2] R. J. Cence *et al.*, Nucl. Instrum. Methods, **138**, 245 (1976).

[3] M. Derrick *et al.*, Phys. Rev. D **17**, 1 (1978).

[4] The dashed curve indicates the $\overline{W^2}$ dependence of $\langle h^- \rangle$ observed in inelastic $\pi^- p$ interactions, where W^2 is defined here as the $\pi^- p$ center-of-mass energy squared. The following data were used to obtain the curve: For $W^2 = 7.47$ GeV^2: M. S. Ainutdinov *et al.*, Zh. Eksp. Teor. Fiz. **47**, 100 (1964) [Sov. Phys.-JETP **20**, 69 (1965)]; A. Citron *et al.*, Phys. Rev. **144**, 1101 (1966); M. L. Perl *et al.*, *ibid.* **132**, 1252 (1963). For $W^2 = 19.67$ GeV^2: M. Bardadin *et al.*, Report No. JINR511/6 – 1964 (unpublished) [as referenced in E. Bracci *et al.*, CERN Report No. CERN/HERA 72–1 (unpublished)]; W. Galbraith *et al.*, Phys. Rev. **138**, B913 (1965); S. Brandt *et al.*, Phys. Rev. Lett. **10**, 413 (1963). For $W^2 = 38.43$ GeV^2: G. W. Brandenburg *et al.*, Nucl. Phys. **B16**, 287 (1970); K. J. Foley *et al.*, Phys. Rev. Lett.

11, 425 (1963); S. P. Denisov *et al.*, Phys. Lett. **36B**, 528 (1971). For $W^2 = 47.8$ GeV^2: J. W. Elbert *et al.*, Nucl. Phys. **B19**, 85 (1970); S. P. Denisov *et al.*, Phys. Lett. **36B**, 528 (1971). For $W^2 = 75.96$ GeV^2: O. Balea *et al.*, Phys. Lett. **39B**, 571 (1972).

[5] In a separate analysis of this same $\bar{\nu}$-nucleus exposure which separated the data in terms of interactions off neutron and proton targets, it was found that $\langle h^- \rangle = 2.0 \pm 0.3$ for the neutron sample and $\langle h^- \rangle = 1.7 \pm 0.1$ for the proton sample. [J. P. Berge *et al.*, Report No. FERMILAB-Pub-78/68-EXP (unpublished)]. We also note that for $P_{\text{inc}} = 40$ GeV/c, $\langle h^- \rangle$ for $\pi^- n$ interactions is 10% higher than $\langle h^- \rangle$ for $\pi^- p$ interactions (see O. Balea *et al.*, Ref. 4).

[6] J. W. Chapman *et al.*, Phys. Rev. **D14**, 5 (1976).

[7] L. Hand, in *Proceedings of the International Symposium on Lepton and Photon Interactions at High Energy, Hamburg, 1977*, edited by F. Gutbrod (DESY, Hamburg, 1977).

[8] When we fit to $dN/dP_t^2 \propto e^{-BP_t^2}$ we obtain $B = 9.50 \pm 0.46$ (GeV/c)$^{-2}$ (χ^2/ND = 34.2/5) and $B = 7.09 \pm 0.53$ (GeV/c)$^{-2}$ (χ^2/ND = 13.6/5) in the range $4 \leqslant W^2 < 20$ GeV^2 and $20 \leqslant W^2 < 100$ GeV^2, respectively.

[9] W. D. Shepard *et al.*, Phys. Rev. Lett. **27**, 1164 (1971).

[10] For $\pi^- n \to \pi^- X$ we used data for $\pi^+ p \to \pi^+ X$ at 16 GeV/c: J. V. Beaupré *et al.*, Phys. Lett. **37B**, 432 (1971).